Efficient Ion Exchange of H^+ for Li^+ in $(Li_{0.30}La_{0.57}\square_{0.13})TiO_3$ Perovskite in Water: Protons As a Probe for Li Location

Anthony Boulant,[‡] Pierre Maury,[†] Joël Emery,[‡] Jean-Yves Buzare,[‡] and Odile Bohnke*[,†]

Laboratoire des Oxydes et Fluorures (UMR 6010 CNRS), and Laboratoire de Physique de l'Etat Condensé (UMR 6087 CNRS), Institut de Recherche en Ingénierie Moléculaire et Matériaux Fonctionnels (FR 2575 CNRS), Université du Maine, Avenue O.Messiaen, 72085 Le Mans Cedex 9, France

Received January 15, 2009. Revised Manuscript Received March 12, 2009

The property of the lithium lanthanum titanate $(Li_{3x}La_{2/3-x}\square_{1/3-2x})TiO_3$ (or LLTO) to exchange protons for lithium has been used to prepare exchanged titanates and indirectly localize Li in the perovskite structure. The exchange reaction has been carried out in ultrapure water to follow the rate of exchange by measuring the pH of the solution. This study shows that a topotactic exchange reaction takes place in LLTO powder that leads to a novel perovskite phase where lithium ions are partially substituted by protons. The rate of exchange depends on the exchange reaction temperature. In the oxide with a high rate of exchange, three types of protons with different environments are clearly detected by ^1H MAS NMR. According to the crystallographic structure of LLTO and to the different basic character of these protons linked to oxygen, it has been possible to propose a location of each type of protons in the structure. The protons are mainly linked to oxygen O3 and to oxygen O2 in the structure and in a very small proportion to oxygen O1. To observe correlation between ^1H nuclei, homonuclear dipolar recoupling BABA and exchange sequence were used. Finally, if we assume that in the exchanged oxides the protons have the same location as the Li^+ ions in LLTO, it is then possible to propose a location of these Li^+ ions and to give an interpretation of the ^7Li NMR spectra.

Introduction

The titanium-based perovskite phase $(Li_{3x}La_{2/3-x}\square_{1/3-2x})TiO_3$ has attracted much attention since the papers of Belous et al. in 1987[1] and Inaguma et al. in 1993[2] who reported a bulk lithium conductivity as high as 10^{-3} S·cm^{-1} at room temperature. This is one of the highest crystalline lithium-ion conductors reported in the literature. Ion migration occurs through the conduction paths formed by Li^+ ions and vacancies $\square$, present in the A-sites of the ABO_3 perovskite structure. To go from one A-site to the next available one, Li^+ has to pass through a bottleneck made of four oxygen ions. Structural data have been published by Fourquet et al.[3] and Robertson et al.[4] These authors agree well to say that a pure solid solution exists only in the composition range $0.04 < x < 0.14$. We recall that the structural model, obtained from the powder X-ray diffraction (XRD) patterns analysis, consists of a tetragonal distortion of the cubic ABO_3 perovskite unit cell with $a = b \approx 3.87$ Å and $c \approx 2a$, with a $c/2$ distortion decreasing for high lithium content. The space group has been determined as *P*4/*mmm*. This space group does not allow a tilting of the TiO_6 octahedra. Recently, Inaguma et al.[5] proposed another space group, *Cmmm*, which allows such a tilting and is certainly more realistic. However, both structural models show that these compounds are disordered crystalline materials as shown by Fourquet et al. using XRD and HREM (high-resolution electron microscopy) techniques.[3] Two kinds of disorders have been mentioned in these studies. One disorder is characterized by the distribution of La^{3+} ions among the sites 1a (0,0,0) and 1b (0,0,1/2) of the structure. The 1a sites are preferentially occupied by La^{3+} ions (around 85% of the site occupancy), although the 1b sites are much less occupied by these ions (around 30% of the site occupancy only). This disorder implies the doubling of the *c* axis parameter. Another disorder exists in the stacking of the 1a (La^{3+}-rich) and 1b (La^{3+}-poor) layers, leading to antiphase domains. This disorder is characterized by a broadening of the (*h*,*k*,*l*) peaks of the XRD patterns, with $l = 2n + 1$.[3]

In this microstructured system the mobility of the Li^+ ions was studied both by impedance spectroscopy[6,7] and by nuclear magnetic resonance (NMR).[8−14] The neutron diffraction experiments were not so conclusive regarding the location of the mobile Li^+ ions in the structure, even at low temperature.

To afford new information on the location of lithium ions in LLTO, we performed conductivity and NMR experiments

* Corresponding author. Tel.:33-2-43 83 33 54. Fax: 33-2-43 83 35 06. E-mail: odile.bohnke@univ-lemans.fr.
† Laboratoire des Oxydes et Fluorures (UMR 6010 CNRS).
‡ Laboratoire de Physique de l'Etat Condensé (UMR 6087 CNRS).

(1) Belous, A. G.; Novitskaya, G. N.; Polyanetskaya, S. V.; Gornikov, Y. I. *Zh. Neorg. Khim.* **1987**, *32*, 283.
(2) Inaguma, Y.; Chen, L.; Itoh, M.; Nakamura, T.; Uchida, T.; Ikuta, H.; Wakihara, M. *Solid State Commun.* **1993**, *86*, 689.
(3) Fourquet, J. L.; Duroy, H.; Crosnier-Lopez, M. P. *J. Solid State Chem.* **1996**, *127*, 283.
(4) Roberston, A. D.; West, A. R.; Ritchie, A. G. *Solid State Ionics* **1997**, *104*, 1.
(5) Inaguma, Y.; Katsumata, T.; Itoh, M.; Mori, Y. *J. Solid State Chem.* **2002**, *166*, 67.
(6) Bohnké, O.; Bohnké, C.; Fourquet, J. L. *Solid State Ionics* **1996**, *91*, 21.
(7) Mazza, D.; Ronchetti, S.; Bohnké, O.; Duroy, H.; Fourquet, J. L. *Solid State Ionics* **2002**, *149*, 81.

10.1021/cm900129u CCC: $40.75
Published on Web 05/01/2009

on "LLTO" perovskite after exchange of Li^+ by H^+. The exchange reaction has been performed in pure water to carefully follow the rate of the exchange reaction. The present work has been carried out on $Li_{0.30}La_{0.57}TiO_3$ synthesized by solid state reaction (SSR). The acronym LLTO will refer, in this paper, to the particular composition of the solid solution $Li_{0.30}La_{0.57}TiO_3$, which shows the highest ionic conductivity.

Experimental Section

Preparation of LLTO Powder. The lithium lanthanum titanate, $Li_{0.30}La_{0.57}TiO_3$, was prepared by reacting stoichiometric amounts of dried La_2O_3, Li_2CO_3, and TiO_2, at 850 °C for 4 h, followed by heating at 1150 °C for 30 h with two intermediate grindings. The details of the synthesis procedure have been reported previously.[3]

Ionic Exchange of H^+ for Li^+ on LLTO Powder. The ionic exchange of H^+ for Li^+ was performed by treating 1 g of the parent oxide, $Li_{0.30}La_{0.57}TiO_3$, in 100 mL aliquots of either ultrapure water or 14 M HNO_3. The experiments were carried out under constant stirring either at room temperature or at 70 °C. The duration of the exchange was varied from 24 to 60 h. After reaction, the powder was separated from the solution by filtration on solid filter (10 μm porosity) and washed. The resultant powder was dried one night in an oven at 120 °C to take off residual adsorbed water.

Characterization of the Powder after Exchange. To characterize the powder after ionic exchange, XRD, thermogravimetric (TG) analysis, impedance spectroscopy, and magic angle spinning nuclear magnetic resonance (MAS NMR) were used.

Powder XRD patterns were recorded at room temperature with a Philips X'Pert PRO diffractometer (Cu Kα radiation). For the structural analysis, slow scan patterns were recorded at room temperature in the 2θ range from 8 to 120° with an increment step of 0.0167° and a collecting time of 7 h 33 min. The XRD patterns were analyzed by the Rietveld method, using FULLPROF software.[15]

Thermal analysis of the proton-exchanged derivatives was done using a TA Instruments SDT 2960 system, with a heating rate of 5 °C/min under a flowing argon atmosphere.

The NMR spectra were recorded with a Bruker Avance 300 spectrometer working at a frequency of $\nu_0 = 116.64$ MHz for ^{7}Li and $\nu_0 = 300.13$ MHz for ^{1}H. The experiments were performed on powdered samples spinning at the magic angle with a standard 4 mm MAS probe. ^{7}Li spectra were referenced from LiCl saturated solution, and the proton ones were referenced from TMS. The DMFIT software was used to fit the spectra and obtain the line widths, the peak positions (in Hz or ppm), and the percentage of each contribution.[16] The $\pi/2$ pulse duration was 4 μs for both nuclei. For the ^{1}H nucleus, the recycle time was 200 s and the spectral width 10 kHz, and 32 scans were accumulated. For the ^{7}Li nucleus, the recycle time was 100 s and the spectral width 10 kHz, and 8 scans were accumulated. In a first step, MAS one-dimensional (1D) pulse experiments were performed on ^{7}Li and ^{1}H nuclei with frequency rotation $\nu_R = 10$ kHz. For the ^{7}Li, the one-pulse sequence was performed with a saturation process. A Hahn echo,[17−19] with an echo delay equal to 10 μs, was used for the ^{1}H nucleus, with a saturation process. To observe correlation between ^{1}H nuclei, homonuclear dipolar recoupling BABA sequence[20−22] was used in MAS with both frequency dimensions synchronized to the rotation frequency. The BABA sequence allows the recoupling of the dipolar interaction, which is averaged by MAS. Two-dimensional (2D) ^{1}H NMR exchange[23] experiments were also carried out. The MAS spectrum is correlated to itself after a given mixing time. During the mixing time, the system can evolve because either the ions jump from one site to another one or its environment changes. If an exchange process between two sites exists, peaks appear out of the diagonal.

Electrical Conductivity Measurement. The electrical conductivity measurements were performed on two dense pellets after sintering at 1150 °C. The compactness of the pellets was about 98%. One pellet is exchanged in 14 M HNO_3 for 1 week at 70 °C (the rate of substitution was 60%) and the other one is used as sintered. Measurements were carried out by complex impedance spectroscopy in the 10 MHz to 1 Hz frequency range with an applied voltage of 100 mV (rms) using a Solartron 1260 impedance gain phase analyzer with SMART impedance software for data acquisition. The measurements were performed on pellets of 5 mm diameter and 1 mm thickness, with the surfaces coated with sputtered Pt as electrodes. Samples were fixed up in a two-probe cell. Impedance data were obtained in the 25−100 °C temperature range under a pure and dry N_2 atmosphere (<5 ppm of O_2). Samples were allowed to equilibrate for 1 h prior to data acquisition to obtain reproducible spectra.

In this paper, samples will be named in the following manner: (Time of exchange_Exchange medium_Temperature). As an example, 24_H2O_70 is the LLTO sample exchanged in water for 24 h, at 70 °C.

Results

Exchange Reaction and Determination of the Rate of Exchange. The exchange reaction of H^+ for Li^+ in LLTO has been carried out in pure water. This reaction has already been observed in an acidic medium (2 M HNO_3) at 60 °C by Bhuvanesh et al.[24] The advantage of using a neutral medium such as water is that we can follow the pH of the solution as exchange occurs; this is not possible in an acidic medium into which proton concentration is very high. Figure 1 shows the evolution of the pH of the ultrapure water as a function of time during reaction between the powder and

(8) Emery, J.; Buzaré, J. Y.; Bohnké, O.; Fourquet, J. L. *Solid State Ionics* **1997**, *99*, 41.
(9) Bohnké, O.; Emery, J.; Véron, A.; Fourquet, J. L.; Buzaré, J. Y.; Florian, P.; Massiot, D. *Solid State Ionics* **1998**, *109*, 25.
(10) Emery, J.; Bohnké, O.; Fourquet, J. L.; Buzaré, J. Y.; Florian, P.; Massiot, D. *J. Phys.: Condens. Matter* **1999**, *11*, 10401.
(11) Emery, J.; Bohnké, O.; Fourquet, J. L.; Buzaré, J. Y.; Florian, P.; Massiot, D. C. R. *Compte Rendu de l'Académie des Sciences, Chimie* **2001**, *4*, 845.
(12) Emery, J.; Bohnké, O.; Fourquet, J. L.; Buzaré, J. Y.; Florian, P.; Massiot, D. *J. Phys. Condens. Matter* **2002**, *14*, 523.
(13) Bohnké, O.; Emery, J.; Fourquet, J. L. *Solid State Ionics* **2003**, *158*, 119.
(14) Bohnké, O.; Emery, J.; Fourquet, J. L.; Badot, J. C. In *Recent Developments in Solid State Ionics*; Pandalai, S. G., Ed.; Transworld Research Network Publishers: Trivadrum (India), 2003; Vol. 1, p 47.
(15) Rodriguez-Carvajal, J. *FULLPROF program: Rietveld Pattern Matching Analysis of Powder Patterns*; ILL: Grenoble, 1990.
(16) Massiot, D.; Fayon, F.; Capron, M.; King, I.; Le Calvé, S.; Alonso, B.; Durand, J.-O.; Bujoli, B.; Gan, Z.; Hoaston, G. *Magn. Reson. Chem.* **2002**, *40*, 70.
(17) Hahn, E. L. *Phys. Rev.* **1950**, *80*, 580.
(18) Lowe, J. *Bull. Am. Phys. Soc.* **1957**, *2*, 344.
(19) Hartmann, S. R.; Hahn, E. L. *Phys. Rev.* **1962**, *128*, 2042.
(20) Schnell, I.; Brown, S. P.; Low, H. L.; Ishida, H.; Spiess, H. W. *J. Am. Chem. Soc.* **1998**, *120*, 11784.
(21) Brown, S. P.; Spiess, H. W. *Chem. Rev.* **2001**, *101*, 4125.
(22) Schnell, I. *Prog. Nucl. Magn. Reson. Spectrosc.* **2004**, *45*, 145.
(23) Jeener, J.; Meier, B. H.; Bachman, P.; Ernst, R. R. *J. Chem. Phys.* **1979**, *71*, 4546.
(24) Bhuvanesh, N. S. P.; Bohnké, O.; Duroy, H.; Crosnier-Lopez, M. P.; Emery, J.; Fourquet, J. L. *Mater. Res. Bull.* **1998**, *33*, 1691.

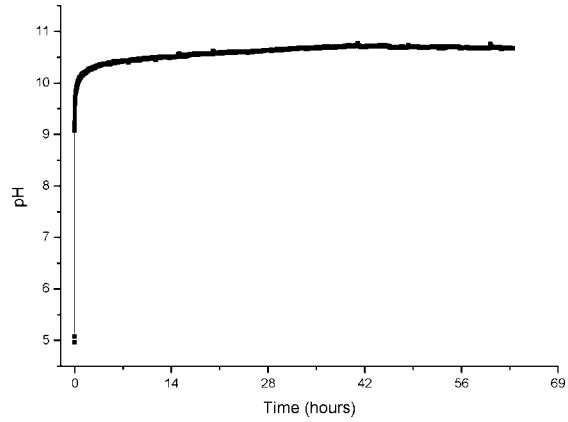

Figure 1. Evolution of pH during the exchange process of LLTO in ultrapure water at 70 °C (sample called 60_H2O_70). The powder is introduced at $t = 0$.

the solution at 70 °C. From the initial pH of water (pH = 5) a sudden increase is observed immediately after the introduction of LLTO powder in the solution. In <1 min the pH reaches 9.3, indicating that proton concentration decreases in the solution. Afterwards, a slow increase of pH, from 9.3 to 10.7, is recorded, which stabilizes after 30 h of reaction. It is worth noting that the same behavior is observed at 25 °C and the pH stabilizes at 10.5 after 30 h of reaction. This experiment clearly shows that protons are consumed during the exchange reaction, yielding to an alkaline solution. As protons are consumed, the equilibrium

$$2H_2O \leftrightarrow H_3O^+ + OH^- \quad (1)$$

is shifted to the right-hand side and water decomposes. The free protons enter the framework of LLTO and OH^- ions are formed, increasing the pH of the solution. The neutrality of the solution is ensured by the Li^+ ions coming from LLTO which have been detected in the solution by flame spectrometry. This experiment shows that an exchange reaction of H^+ for Li^+ has taken place in LLTO and that an acidic medium and then high proton activity in solution are not required for the exchange reaction to occur, contrary to what has been described by Simon et al.[25] The exchange reaction can then be written as follows:

$$Li_{0.30}La_{0.57}TiO_3 + yH_2O \rightarrow (Li_{0.30-y}H_y)La_{0.57}TiO_3 + yLi^+ + yOH^- \quad (2)$$

This reaction can be either total, when $y = 0.3$ or partial when $y < 0.3$ (for this particular composition of LLTO).

Figure 2 shows the XRD patterns of LLTO powder recorded at room temperature after synthesis (a) and of the powder after exchange at 70 °C for 24 h in water (or 24_H2O_70 sample) (b). The patterns are similar, indicating that the exchange reaction proceeds via a topotactic reaction. Both patterns could be indexed in a tetragonal cell.

Figure 3 shows the XRD pattern of 24_H2O_70 sample and its refinement with FULLPROF software.[15] The structure refinement indicates a very slight increase of the lattice parameters after exchange (Table 1). However, such a small variation may be not significant.

(25) Simon, D. R.; Kelder, E. M.; Wagemaker, M.; Mulder, F. M.; Schoonman, J. *Solid State Ionics* **2006**, *177*, 2759.

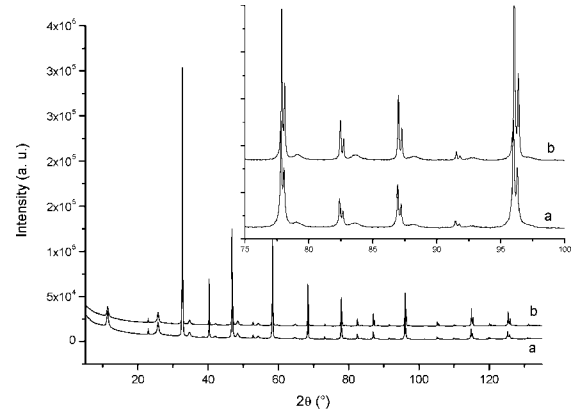

Figure 2. Powder XRD patterns of samples: (a) after synthesis; (b) after exchange for 24 h in ultrapure water at 70 °C.

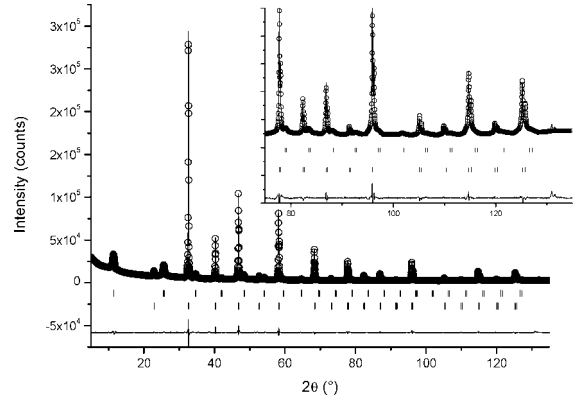

Figure 3. Observed (○), calculated (−), and difference plots of the Rietveld refinement of the 24_H2O_70 sample XRD spectrum. Reflection positions are shown as vertical bars.

Two techniques were used to obtain the rate of substitution: TG analysis and ^7Li NMR both performed on the powder after exchange. These experiments were carried out after separation of the powder from the water as described in the experimental procedure.

TG curves obtained in the temperature range from 25 to 1000 °C on LLTO powder after synthesis (a) and on the powder after exchange at 70 °C for 24 h (b) are shown in Figure 4. After synthesis, LLTO is thermally stable in the temperature range investigated; no weight loss is observed (curve a). On the other hand, the TG curve obtained on the exchange powder reveals two weight losses: a first weak one in the 50−200 °C temperature range and a second one around 300−500 °C. The first one can be ascribed to adsorbed water; this is confirmed by the presence of an endothermic peak in the DTA curve. The amount of adsorbed water on the surface of the powder is small, of the order of 0.02 wt %. The second weight loss indicates that the exchanged phase starts dehydrating to yield a novel phase of composition $Li_{0.30-y}La_{0.57}TiO_{3-y/2}$. The weight loss is in good agreement with the evolution of H_2O according to the following reaction:

$$(Li_{0.30-y}H_y)La_{0.57}TiO_3 \rightarrow Li_{0.30-y}La_{0.57}TiO_{3-y/2} + y/2H_2O \quad (3)$$

From the weight loss recorded by thermal analysis, it is possible to determine the rate of exchange. Indeed, the dehydration of the totally exchanged oxide ($H_{0.3}La_{0.57}TiO_3$),

Table 1. Unit Cell Parameters Obtained after Rietveld Refinement with FULLPROF Software[a]

name	solution	lattice parameter		R_{bragg}	R_p	R_{wp}	R_{exp}	κ^2
		a (Å)	c (Å)					
24_HNO3_70	HNO_3 (70 °C)	3.87772(3)	7.75927(3)	1/2.42	8.51	8.51	2.96	8.29
24_H2O_70	ultrapure water	3.87959(7)	7.75992(35)	1.92/2.30	9.4	8.95	2.96	9.14
LLTO_SSR		3.87653(7)	7.75493(6)	5.41/8.65	11.9	11.8	3.08	14.7

[a] There are two R_{bragg} values for LLTO_SSR (sample after solid state reaction synthesis) because two phases are used for the refinement as explained in ref 3.

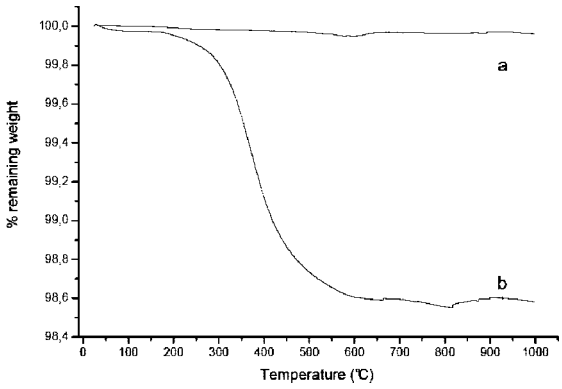

Figure 4. TG curve in the temperature range from 25 to 1000 °C on LLTO powder after synthesis (a) and after exchange in water, 70 °C, for 24 h (b). The temperature rate was 5 °C·min^{-1}.

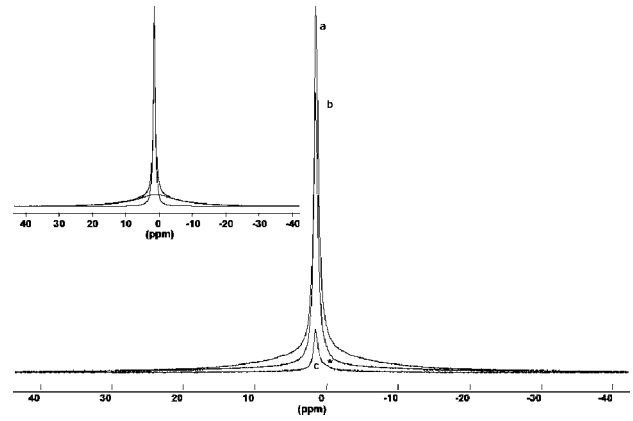

Figure 5. ^{7}Li NMR MAS (10 kHz) spectra of LLTO powder after synthesis (a), after exchange in water at 25 °C for 24 h (b), and after exchange in water at 70 °C for 24 h (c). Spectra have been normalized to the powder weight. The insert shows the reconstruction of curve (a). * is for impurity (1% of lithium total).

which can also be written as $(La_{0.57}TiO_{2.7}(OH)_{0.3})$, leads to the novel phase $La_{0.57}TiO_{2.85}$, which is metastable and decomposes into $La_2Ti_2O_7$ and $La_4Ti_9O_{24}$ according to the following reaction:[23]

$$La_{0.57}TiO_{2.7}(OH)_{0.3} \rightarrow 0.113La_2Ti_2O_7 + 0.086La_4Ti_9O_{24} + 0.15H_2O \quad (4)$$

When exchange is total, the theoretical weight loss is 1.53%. According to the weight loss recorded in TG curves, the rate of substitution of LLTO powder in water at 25 °C is found to be 18% for 24 h of exchange. The rate of substitution at 70 °C is found to be 85% and 90% for 24 and 60 h of exchange, respectively. It is worth noting that we never succeeded in obtaining total exchange in water, whatever the temperature.

Figure 5 presents ^{7}Li MAS (10 kHz) NMR spectra obtained at room temperature on LLTO powder after synthesis (a), on the powder after exchange in water at 25 °C for 24 h (b), and on the powder after exchange in water at 70 °C for 24 h (c). The spectra were normalized according to the weight of the sample used in the experiments. It can be observed that the intensity of the line, which is proportional to the number of ^{7}Li nuclei, decreases as exchange occurs, confirming that the exchange reaction has taken place in the oxide. From these spectra the rate of substitution can also be determined. A rate of 89% is found for the exchange performed at 70 °C for 24 h, although a much smaller rate of 25% is obtained when exchange is performed at 25 °C for 24 h. ^{7}Li MAS NMR spectra have also been recorded for the sample after 60 h of exchange at 70 °C. A rate of exchange of 92% has been determined. These results confirm the thermal analysis experiments (* indicates a nonexchangeable impurity, which accounts for 2% of total lithium).

Table 2 summarizes the above results obtained with the two methods. We also reported in this table the results obtained after exchange of the same LLTO powder in an acidic medium (14 M HNO_3) at 70 °C after 24 h of exchange. The two methods give similar rates of substitution. It can be observed that it is possible to reach a very high rate of substitution in water solution.

Conductivity of a Pellet after Exchange. Impedance spectroscopy has been performed on a pellet before and after the exchange reaction. In this experiment the exchange has been carried out on a sintered LLTO pellet exchanged in 14 M HNO_3 for 1 week at 70 °C. The rate of substitution was 60%. A decrease of the bulk conductivity of 2 orders of magnitude is observed after exchange going from 3×10^{-3} to 5×10^{-5} S·cm^{-1} at 25 °C for LLTO and the exchanged oxide, respectively. Since the number and charge of the mobile species remain the same after exchange and if we assume that the lithium mobility remains constant, the decrease of conductivity of 2 orders of magnitude can be explained by a strong decrease of the mobility of the protons when they are present in the structure. The exchange process may also reduce the lithium mobility: the protons can act as obstacles to the lithium motion in the perovskite as do La ions.

MAS NMR on Powder after Exchange. ^{7}Li MAS NMR spectra, shown in Figure 5, display only one line whatever the rate of exchange. The insert of Figure 5 shows the reconstructed NMR spectrum of the sample before exchange. We need two components with the same isotropic chemical shift: a broad one that accounts for 53% of the spectrum and a narrow one that accounts for 47%. This result is in agreement with the one obtained previously.[12] The spectrum of the sample after exchange at 25 °C for 24 h (25% of exchange) can be fitted with two components: a broad line that accounts for 46% of the spectrum and a narrow one

Table 2. Rate of Substitution Measured by TGA, ^{7}Li NMR, and Chemical Composition (from TGA Measurement)

name	solution	time (h)	temp (°C)	substitution percentage		composition
				TGA	^{7}Li NMR	
24_HNO3_70	HNO_3	24	70	78	80	$H_{0.23}Li_{0.07}La_{0.57}TiO_3$
24_H2O_70	ultrapurewater	24	70	85	89	$H_{0.25}Li_{0.05}La_{0.57}TiO_3$
24_H2O_25	ultrapurewater	24	25	18	25	$H_{0.05}Li_{0.25}La_{0.57}TiO_3$
60_H2O_70	ultrapurewater	60	70	90	92	$H_{0.27}Li_{0.03}La_{0.57}TiO_3$

Table 3. Characteristics of ^{7}Li NMR Line after Refinement with DMfit Software[a]

	exchange 24 h at 70 °C (89%)			exchange 24 h at 25 °C (25%)			sample without exchange		
no. of component	δ (ppm)	Δ (ppm)	%	δ (ppm)	Δ (ppm)	%	δ (ppm)	Δ (ppm)	%
1	1.51	0.71	60	1.53	0.63	54	1.45	0.73	47
2	1.04	14.16	40	1.5	22.43	46	0.93	14.28	53

[a] δ is the isotropic chemical shift; Δ is the line width. All lines used are Lorentzian ones.

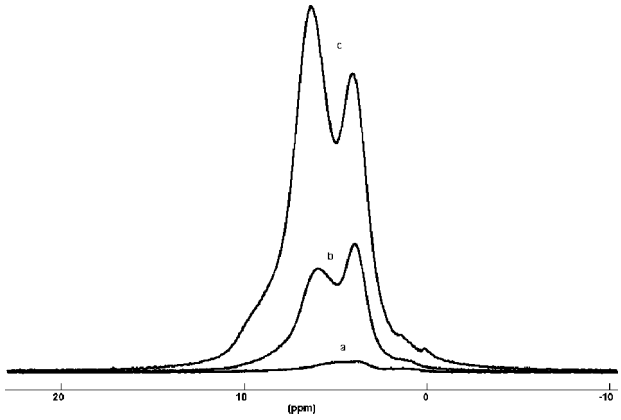

Figure 6. ^{1}H NMR MAS (10 kHz) Hahn Echo spectra of LLTO powder after synthesis (a), after exchange in water at 25 °C for 24 h (b), and after exchange in water at 70 °C for 24 h (c). Spectra have been normalized to the powder weight.

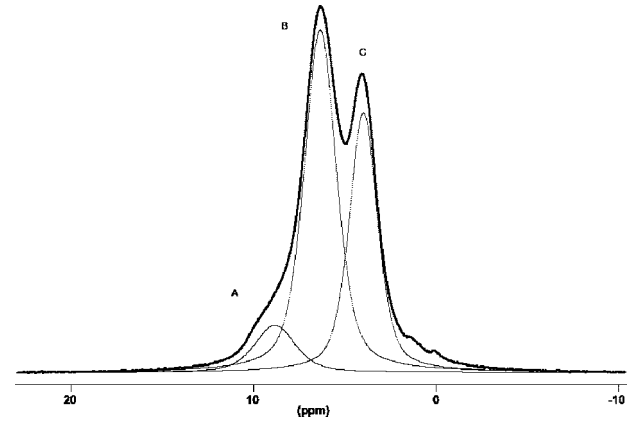

Figure 7. ^{1}H NMR MAS (10 kHz) Hahn Echo spectra recorded on LLTO exchange in water at 70 °C for 24 h (24_H2O_70). The dotted lines are the results of the fitting procedure.

that accounts for 54%. When exchange is performed at 70 °C for 24 h (89% of exchange), the narrow line accounts for 60%. Table 3 summarizes the results of ^{7}Li MAS NMR. In this table, it can be observed that the width of the narrow line, located at 1.5 ppm, remains constant, whereas its relative intensity increases as substitution rate increases: from 47% before exchange to 54% for 25% of exchange and finally to 60% for 89% of exchange. Table 3 does not take into account the nonexchangeable impurity, mentioned before.

Figure 6 presents ^{1}H MAS (10 kHz) NMR spectra, obtained with Hahn Echo pulse sequence, for the three samples: before exchange (spectrum a), after exchange at 25 °C for 24 h (spectrum b), and after exchange at 70 °C for 24 h (spectrum c). As expected, when the exchange rate increases, the intensity of the ^{1}H NMR spectrum increases. However, when ^{7}Li NMR spectra show only one line (fitted with two components with the same isotropic chemical shift), the ^{1}H NMR spectra reveal three lines, located at different isotropic chemical shifts, the intensity of which depends strongly on the rate of substitution. It has to be noted that the contribution located at 0 ppm is attributed to residual ethanol traces and does not belong to the exchange material. It will not be considered in the discussion part of the paper. The reconstruction of the ^{1}H NMR spectrum, as shown in Figure 7, is made of a small and broad line located at 8.83 ppm (A) and of two intense and narrow lines located at 6.35 ppm (B) and 3.98 ppm (C). Both intense lines, B and C, were fitted with only one component. The small and broad line A, which is observed only for a high exchange rate, is fitted with a pure Gaussian component for the high-exchanged sample and low-exchanged sample, suggesting that a distribution of ^{1}H nucleus sites is responsible for this line.

Table 4 summarizes the results of ^{1}H MAS NMR for the four exchanged samples with the line position, the line width, and the relative intensity of each of the lines. The line shape used for fitting is a pseudo-Voigt profile, which is a superposition of a Gaussian line with the percentage xG and a Lorentzian one with the percentage (1 − xG). Therefore, the Lorentzian line (xG = 0), pseudo-Voigt line (xG = 0.5), and Gaussian line (xG = 1) have been used. It can be observed that line widths and relative intensities of the lines depend on the exchange rate (samples 24_H2O_25 and 24_H2O_70). When lines A and C remain at the same position, line B shifts to higher ppm values, when the substitution rate increases.

The same spectrum, with three lines, located at the same positions as previously described, is obtained when exchange is performed in an acidic medium (14 M HNO_3), as shown in Figure 8. Table 4 shows that ^{1}H NMR lines characteristic of samples exchanged in nitric acid and water are similar. This result indicates that the protons are located in the same environment whatever the medium used for the exchange, i.e., water or acid.

Figure 9 shows the 2D MAS homonuclear ^{1}H−^{1}H NMR spectra obtained at 10 kHz with one cycle of the dipolar

Table 4. Characteristics of ^{1}H NMR Lines after Refinement with DMfit Software for Different Exchanged Samples (18%, 85%, 90%, and 78%, respectively)[a]

	exchange H_2O 24 h at 25 °C				exchange H_2O 24 h at 70 °C				exchange H_2O 60 h at 70 °C				exchange HNO_3 24 h at 70 °C			
line	δ	Δ	%	xG	δ	Δ	%	xG	δ	Δ	%	xG	δ	Δ	%	xG
A	8.8	2.09	3.0	1	8.83	2.61	9.4	0.5	8.79	2.73	9.2	0.5	8.81	2.44	8.0	0.5
B	5.96	2.37	57.0	0.5	6.35	2.08	54.3	0.5	6.31	2.1	53.0	0.5	6.29	2.11	55.4	0.5
C	3.88	1.48	40.0	0.5	3.98	1.83	36.3	0.5	3.98	1.8	37.8	0.5	3.96	1.7	36.6	0.5

[a] δ is the isotropic chemical shift (ppm); Δ is the line width (ppm); xG is the percentage of Gaussian line in the Voigt line.

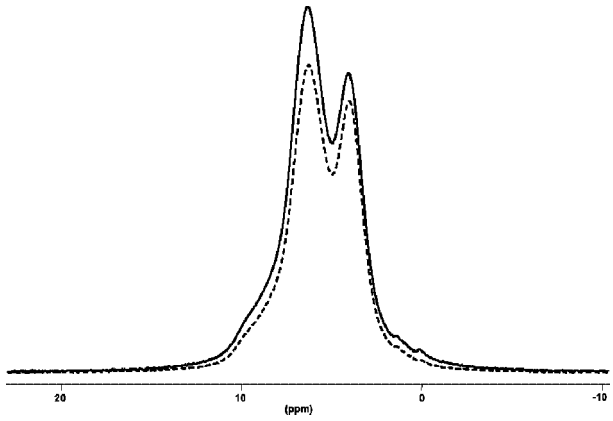

Figure 8. Normalized ^{1}H NMR MAS (10 kHz) Hahn Echo spectra recorded on LLTO after exchange in water (24_H2O_70) (solid line) and in 14 M HNO_3 (24_HNO3_70) (dashed line) at 70 °C for 24 h.

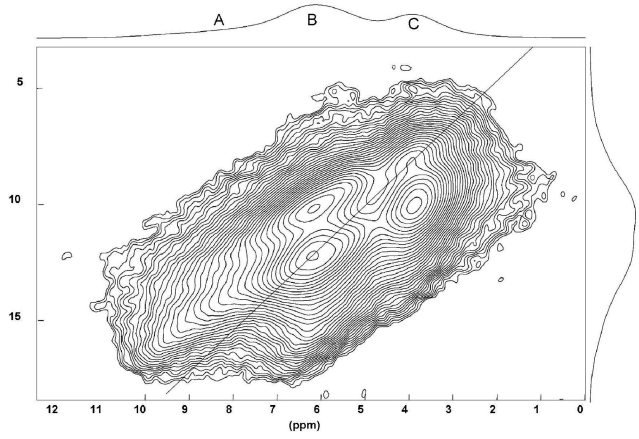

Figure 9. 2D Double Quantum MAS homonuclear ^{1}H−^{1}H NMR spectra obtained at 10 kHz with one cycle of the dipolar recoupling BABA sequence. The vertical axis is the double quantum axis (DQ). The horizontal axis is the single quantum axis corresponding to the MAS spectra filtered by the DQ. The line corresponds to the DQ diagonal.

recoupling BABA sequence. This 2D spectrum evidences some autocorrelation B−B and C−C between equivalent sites, and intercorrelation between sites B and C. It means that equivalent sites B are close to one another, as are sites C. Moreover, sites B and sites C are near each other. So all hydrogen sites are in the proximity of the others. There may be another intercorrelation between sites A and B. But it is not so well-defined because of large spreading and a small relative percentage of line A. It is also difficult to make any conclusions about the correlation of line A.

Figure 10 shows the 2D ^{1}H exchange spectra for sample exchanged 24 h in water at 70 °C, with several mixing times. For 1 ms mixing time, only on diagonal peaks A−A, B−B, and C−C are observed on the 2D card but no peak is observed out of the diagonal. This means that the protons remain at their initial site and do not perform any jump process. For the 10 ms mixing time, intercorrelations A–B and B–C begin to appear as peaks located out of the diagonal. The autocorrelations A–A, B–B and C–C are always observed on the diagonal. This means that the protons jump between A and B sites, on one hand, and between B and C sites, on the other hand. For longer times (50 and 100 ms) the autocorrelations B−B and C−C and the intercorrelations A−B, A−C, and B−C are present. The A−A autocorrelations seem to disappear, owing to the high relative abundance of sites B and C.

Discussion

From these experimental results it can be observed that the exchange reaction of H^+ for Li^+ in LLTO powder does not require an acidic medium and then high proton activity in solution to occur. This shows that the LLTO perovskite phase, as a powder, is not stable in the presence of water at 70 °C and that it leads to a novel perovskite phase $(Li_{0.30-y}H_y)La_{0.57}TiO_3$ that decomposes around 300 °C. At room temperature this process is much slower since only 25% of exchange is observed.

Despite many attempts and the use of different techniques such as neutron diffraction and NMR experiments, the exact location of the Li^+ ions in LLTO structure has never been definitively established and is always a matter of discussion. This is due partly to the high mobility of these ions in this oxide. Another difficulty in ^{7}Li NMR experiments lies in the small chemical shift range for lithium and it is often difficult to distinguish resonances with varying local environments of this nucleus. Further, the NMR spectra are particularly difficult to interpret when powder samples are involved and when there are multiple sites in the unit cell giving rise to overlapping spectra. This is clearly observed in the ^{7}Li MAS NMR spectra in Figure 5, which shows only one line. However, the experimental spectrum can be reconstructed with two Lorentzians, as shown in the insert of Figure 5 and in Table 3. These two lines have approximately the same chemical shift but strongly differ by their widths, one is narrow (ca. 0.7 ppm) and the other one is very broad (ca. 15−20 ppm). The presence of these two lines suggests the existence of two kinds of lithium ions in the structure as discussed in our previous papers.[9−14]

The possibility of exchanging lithium ions by protons may afford some new information on the lithium location if we assume that the lithium ions are replaced by protons with the same position. As the exchange is a topotactic reaction, this assumption seems to be realistic. Indeed, the protons have some interesting properties: the ^{1}H nuclei are more sensitive to chemical shift; besides, they are less mobile than

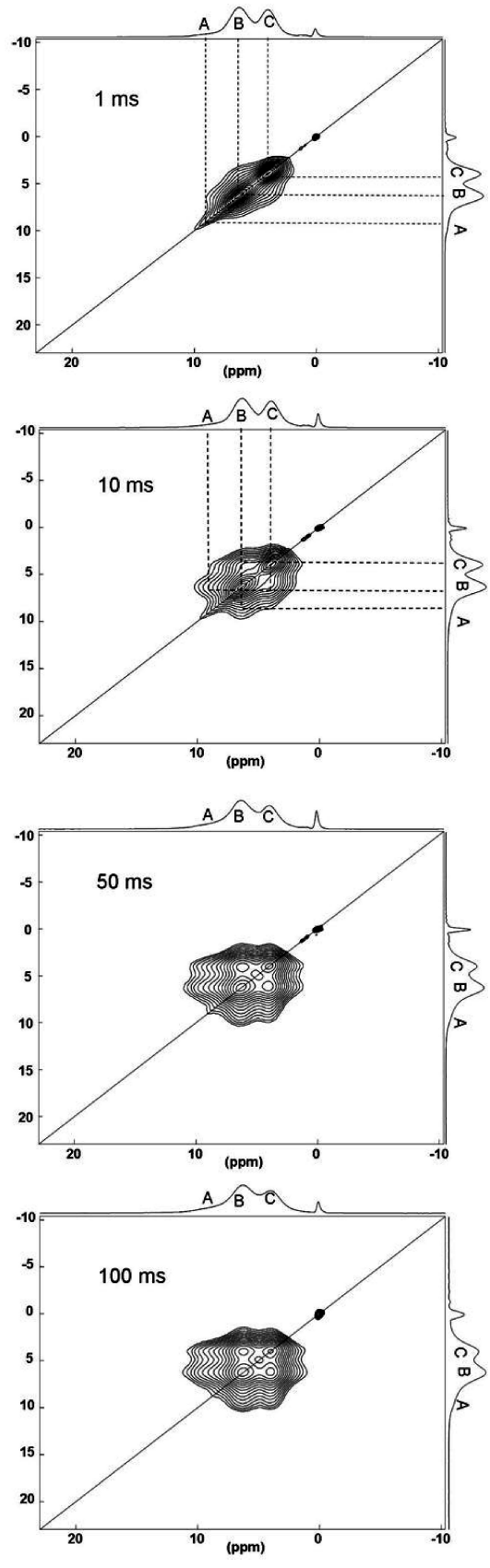

Figure 10. ^{1}H 2D MAS exchange NMR spectra of sample 24_H2O_70 for different mixing times. The vertical axis corresponds to the first dimension before the mixing time, and the horizontal axis is the single quantum axis corresponding to the MAS spectra. For 1 ms of mixing time, dashed lines represent autocorrelations, whereas for 10 ms, they indicate intercorrelations.

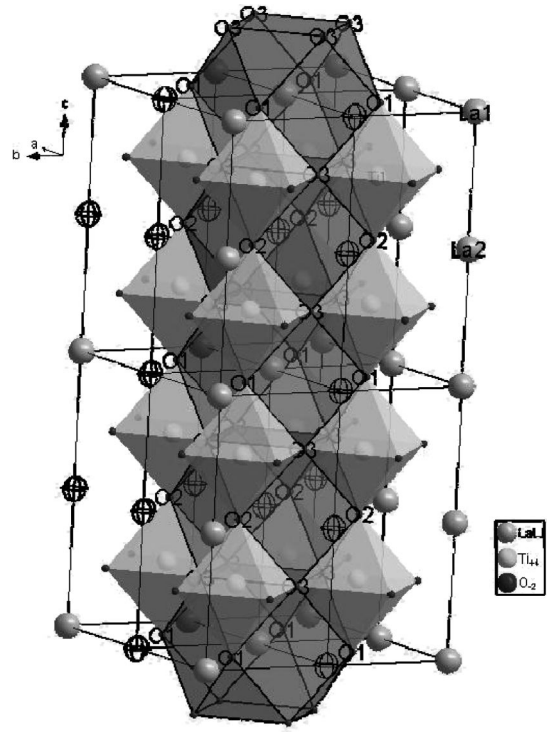

Figure 11. LLTO structural model (*P*4/*mmm*). Unfilled circles are for vacancy or lithium ions.

the lithium ions in LLTO and then the motional averaging will be less active for the protons than for the lithium ions which are very mobile. As described previously, the ^{1}H NMR spectra reveal the presence of three different hydrogen environments in the structure corresponding to three lines located at different isotropic chemical shifts. From these three different kinds of hydrogen nuclei, two are predominant (sites B and C) and account for 90% of the total signal, and the third one (site A) has a much lower amount and accounts for only 10% of the ^{1}H NMR signal, for the sample exchanged at 89%. The environments of the mobile nuclei that cannot be distinguished in the case of lithium nuclei can now be distinguished in the case of proton nuclei. Considering the general properties of the nucleus screening, the lower the chemical shift (or the higher the magnetic field), the more screened the nucleus. This means that the proton nucleus responsible of the NMR line with a low chemical shift has high electronic density. Chemically speaking, this means that such a nucleus has basic character. On the other hand, the proton responsible for the NMR line with a high chemical shift should have more acidic character.

It is of interest to relate these different environments to the crystallographic structure of LLTO. Figure 11 shows the structure of LLTO described in the space group *P*4/*mmm*.[3] In this model, TiO_6 octahedra are linked together by corners through oxygen atoms. Eight such octahedra form the perovskite cage, made of 12 oxygen ions, into which either one La^{3+} or one Li^+ or one vacancy resides. In LLTO all the perovskite cages, in the *c* direction, are not equivalent. For two adjacent cages in the *c* direction, one is mostly populated by La^{3+} ions (85% of the site) and the next one is much less populated by this ion (30% of the site). This leads to the presence of different layers in this direction: a La-rich layer (with La^{3+} ions named

La1) and a La-poor layer (with La^{3+} ions named La2). In the La-rich layer, the La^{3+} ions are surrounded by 12 oxygen ions: 4 oxygen ions named O1 and 8 oxygen ions named O3. In the La-poor layer, the La^{3+} ions are also surrounded by 12 oxygen ions: 4 oxygen ions named O2 and 8 oxygen ions named O3. All the oxygen ions are linked to 2 Ti^{4+} ions and to 4 or less La^{3+} ions. According to the different occupancies of La^{3+} ions in these layers, the mean coordination of these three kinds of oxygen ions is different and therefore their electronic density is also different. The oxygen O1, which belongs to the La-rich layer, is more coordinated than the oxygen O3, which is located between a La-rich layer and a La-poor layer, and even more than the oxygen O2, which belongs to the La-poor layer. This implies that the oxygen O1 has a lower electronic density than the oxygen O3, which has an even lower electronic density than the oxygen O2. Consequently, the protons that will be linked to oxygen O2 will have a stronger basic character than the protons linked to oxygen O3. These latter protons will have a stronger basic character than the protons linked to oxygen O1.

It is then possible to associate the three ^{1}H NMR lines to these different protons. Line A could then be ascribed to protons linked to oxygen O1 in the La-rich layer. Since they reside in the La-rich layer, the number of such protons is very small and the NMR signal is weak. Line B could be ascribed to protons linked to oxygen O3. These protons can belong either to the La-poor layer or to the La-rich layer. We can postulate that, as exchange proceeds, the protons first exchange with lithium ions located in the La-poor layer and that after some rate of substitution they will exchange with lithium ions from the La-rich layer. This may explain the shift of line B to a higher chemical shift during exchange. Finally, line C can be ascribed to protons linked to oxygen O2 in the La-poor layer.

During their motion in the $a-b$ direction, the protons in the La-poor layer will move from O3 to O2, then pass through the bottleneck made of 4 oxygens O2, and then go to O3 in the next available A-cage. The motion of the protons in the c direction, through the bottleneck made of 4 oxygens O3 and then to O1, is much less favored, as shown by the small intensity of the NMR line A. We can then postulate that a 2D motion is certainly favored in LLTO at room temperature in the $a-b$ direction. This result agrees well with our previous results[11,12] and those obtained by Mazza et al. who used the concept of bond valence and calculated the bond valence sum (BVS) of Li ions during their travel in the perovskite cage,[7] by Inaguma et al.,[26] and by Kobayashi et al.[27] who used molecular dynamics technique to determine the conduction pathways of lithium ions.

These proton positions are also consistent with the results of 2D MAS homonuclear ^{1}H$-^1$H NMR spectra shown in Figure 9. The distance between protons linked to O3 and protons linked to O2 is less than the value of the a (or b) parameter. Therefore, these protons (responsible for lines B and C) are highly correlated. Furthermore, the protons linked to O3 are distant from each other, of a value corresponding to the a parameter as it is for protons linked to O2. This explains why they are both self-correlated. On the other hand, the protons linked to O1 are distant from each other, of one or several cell parameters a, owing to the small occupancy of protons in the La-rich layer. This explains why the signal is small and why these protons are not or very slightly self-correlated.

The 2D ^{1}H exchange NMR experiment results also confirm the previous description of site B (hydrogen bounded to oxygen O3) and C (hydrogen bounded to oxygen O2) and the above proposed mechanism. Site B exchanges its magnetization with sites A and C. Its position assignment between oxygen O1 and O2 is consistent with this observation. Furthermore, these experiments give a numerical range of the interaction correlation time value (approximately 1 ms), which accounts for the ionic dynamics.

The relative percentage intensities of the three lines of the ^{1}H NMR MAS spectrum measured after 89% of exchange (54% for line B and 36% for line C, as shown in Table 4) have to be compared to the relative percentage of the two components of the ^{7}Li NMR MAS spectrum obtained on LLTO (53% for the broad line and 47% for the narrow one, as indicated in Table 3). The same observation is valuable for other samples exchanged in water or nitric acid (Table 4). Those similar values are in good agreement with our previous assumption that protons are located at the same position as lithium ions in LLTO after exchange. Protons can then be a good probe for the location of Li^+ ions in the LLTO phase. Therefore, it is possible to associate line B of the ^{1}H NMR spectrum to the broad line observed in the ^{7}Li NMR spectrum and then to conclude that these Li^+ ions are close to oxygen O3, which are located between a La-rich layer and a La-poor layer. Moreover, the translation of the B line to the low magnetic field, as exchange rate increases, which are related to protons that are linked to oxygen O3 and that can be located either in the La-poor layer (for low exchange rate) or in the La-rich layer (for high exchange rate), can be related to the broadness of the line observed in ^{7}Li NMR spectrum. A distribution of Li sites linked to oxygen O3 could then be responsible for the broadness of this line. Finally, it is possible to associate line C of the ^{1}H NMR spectrum to the narrow line observed in the ^{7}Li NMR spectrum. These Li^+ ions would be close to oxygen O2, which belong to the La-poor layer of the structure. These findings suggest that the main diffusion path of lithium ions is in the La-poor layer and that these ions migrate through the O2 bottleneck via O3 oxygen ions. The migration in the c direction seems to be more difficult owing to the high occupancy of the La-rich layer.

Conclusions

The protons, present in the perovskite phase after topotactic exchange reaction of LLTO in water, have been used as a probe to locate the Li^+ ions in the perovskite structure. We used the property of LLTO, as a powder, to react with water at high temperature to prepare partially substituted perovskite (up to 89% of exchange). The decrease of proton mobility has been very useful to discriminate different environments, with distinct isotropic chemical shifts. The inserted protons

(26) Yashima, M.; Itoh, M.; Inaguma, Y.; Mori, Y. *J. Am. Chem. Soc.* **2005**, *127*, 3491.
(27) Maruyama, Y.; Ogawa, H.; Kamimura, M.; Kobayashi, M. *J. Phys. Soc. Jpn.* **2006**, *75*, 064602.

reveal then to be useful probes for location of the lithium ions in LLTO structure. As the exchange is topotactic, we can assume that inserted protons have the same location in the structure as lithium ions. According to the crystallographic structure of LLTO and to the ^{1}H MAS NMR spectra obtained on exchanged oxides, the protons and then the lithium ions are found to be close to oxygen O3 and O2 in the structure. The Li^+ ions linked to O2 are certainly responsible for the narrow line observed in the ^{7}Li MAS NMR spectrum and the Li^+ ions linked to O3 are responsible for the broad line. Such location seems to favor a 2D motion of these ions, in the $a-b$ direction, at room temperature. The lithium ions follow then a pathway going from O2 to O2 through the O3 oxygen in the perovskite cage of the structure and passing through the bottleneck made of four oxygens O2.

Acknowledgment. The authors thank A. Bulou for a valuable suggestion.

CM900129U